Phase transition in the Ising ferromagnetic model with fixed spins

A. Labarta
Departamento de Física Fundamental, Universidad de Barcelona, Diagonal 647, 08028-Barcelona, Spain
J. Marro
Departamento de Física Aplicada, Facultad de Ciencias, Universidad de Granada, 18071-Granada, Spain
B. Martinez and J. Tejada
Deparamento de Física Fundamental, Universidad de Barcelona, Diagonal 647, 08028-Barcelona, Spain
(Received 8 July 1987; revised manuscript received 17 December 1987)

The ferromagnetic Ising spin-$\frac{1}{2}$ model in a finite simple-cubic lattice Λ is studied by Monte Carlo methods when two subsets of the lattice sites in Λ, say Ω^+ and Ω^-, contain (the same number of) spins fixed at ± 1, respectively, the global defect concentration being $x \leq 0.25$. We study the thermodynamic properties of the model for different choices of $\Omega = \Omega^+ \cup \Omega^-$. A finite-size-scaling analysis reveals that the transition remains second order with pure critical exponents for regularly spaced defects, the critical temperature varying with the symmetry of Ω. Any small randomness in Ω, however, makes the transition weakly first order; the transition becomes more abrupt for defects located fully at random, and the long-range order is suppressed when the numbers of defects in Ω^+ and Ω^- differ from each other. We also discuss our findings in relation to the random-field and frustration problems.

I. INTRODUCTION

In a series of recent analytical[1,2] and numerical[2–4] studies we were concerned about the modifications which are induced by the presence of quenched (or frozen-in) impurities or defects in the behavior of the pure Ising model. That work motivated the present paper where we are specifically interested in the study of the influence of the symmetry which characterizes the quenched-defect (namely, spins $\frac{1}{2}$ fixed either "up" or "down") distribution on the nature of the involved phase transition. With that aim we shall consider the ferromagnetic Ising model on a simple-cubic lattice, say Λ, with lattice spacing a_0, defined by the Hamiltonian

$$H(\mathbf{s}) = -J \sum_{|\mathbf{x}-\mathbf{y}|=1} s_{\mathbf{x}} s_{\mathbf{y}}, \quad J>0 , \tag{1.1}$$

where $\mathbf{x},\mathbf{y} \in \Lambda$, the sum is over nearest-neighbor pairs, and $\mathbf{s} \equiv \{s_{\mathbf{x}}\}$. The spin variables $s_{\mathbf{x}}$ are in general allowed to have any of two symmetric values, ± 1, as in the pure Ising model, except when $\mathbf{x}$ belongs to a given subset Ω of (fixed) lattice sites in Λ, namely,

$$s_{\mathbf{x}} = \begin{cases} \pm 1 \text{ (stochastic variable) when } \mathbf{x} \in \overline{\Omega} \\ +1 \text{ (fixed value) when } \mathbf{x} \in \Omega^+ \\ -1 \text{ (fixed value) when } \mathbf{x} \in \Omega^- , \end{cases} \tag{1.2}$$

where $\overline{\Omega} \cup \Omega = \Lambda$, $\overline{\Omega} \cap \Omega = \emptyset$, $\Omega^+ \cup \Omega^- = \Omega$, $\Omega^+ \cap \Omega^- = \emptyset$, and Ω^+ and Ω^- contain the same number of lattice sites so that the net magnetization introduced by the defects is zero (this restriction will be raised in one of our studies, however). Our interest is thus on the comparison between the thermodynamic properties of the model for different realizations of Ω.

We shall consider explicitly the following different realizations of the defects sublattice.

Case 1. Ω is a simple-cubic lattice with lattice spacing $2a_0$, so that the defect concentration is $x=0.125$, and Ω^+ and Ω^- are the two (face-centered-cubic) sublattices of Ω with lattice spacing $4a_0$ [cf. Fig. 1(a)]. That is, Ω and Λ have the same symmetry.

Case 2. Ω has a monoclinic symmetry, as shown by Fig. 1(b), and $x=0.125$; positive and negative fixed spins alternate.

Case 3. Ω forms a body-centered-cubic lattice inside Λ, as illustrated by Fig. 1(c), implying that $x=0.25$; positive and negative fixed spins alternate.

Case 4. Ω is a collection of lattice sites whose elements are chosen at random from Λ in order to have a com-

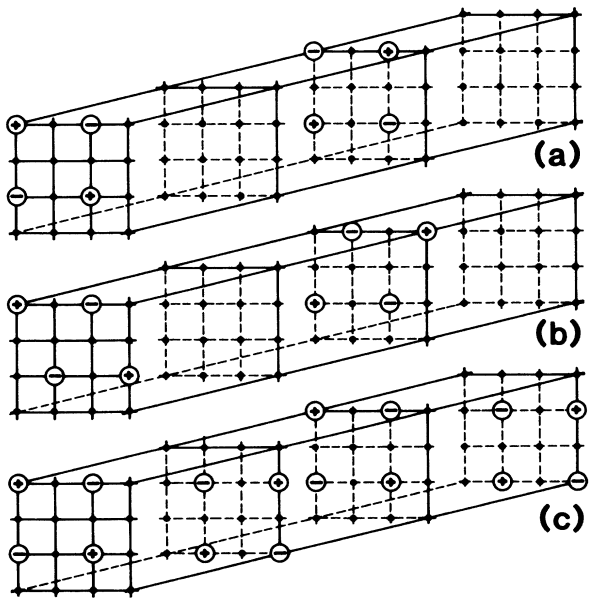

FIG. 1. Defects locations in cases 1 (a), 2 (b), and 3 (c) as defined in Sec. I. The dots represent free spins; the circles ⊕ represent fixed up spins, and the circles ⊖ represent fixed down spins.

pletely random distribution of defects, i.e., one with spherical symmetry; $x=0.1$, 0.125. Ω^+ is also random inside Ω.

We shall report as well on the observed changes when the random locations of the fixed spins in case 4, with $x=0.125$, are progressively constrained (each defect location is selected at random from the lattice sites inside a volume αa_0^3, with α decreasing towards unity) so that one tends (as $\alpha \rightarrow 1$) to the regular distribution in case 1.

The different realizations of Ω are expected to produce noticeable differences in the macroscopic behavior of the system; particularly interesting *a priori* is the comparison between randomly distributed defects (see Refs. 1 and 4 for a bibliography) and the less familiar case (see, however, Refs. 5 and 6 for examples) of regularly fixed spins. The present study is also expected to bear some physical relevance in relation to the random-field Ising (RFI) problem (see Refs. 7 and 8 for instance) given that the situation in (1.2) may be interpreted (e.g., as a consequence of local crystal fields) as caused by a field capable of only three values, 0 and $\pm\infty$, depending on whether it acts on the standard ions in Ω or on the defects in Ω^+ and Ω^-, respectively; our disorder parameter is not the field strength, however, but the defect concentration x and the symmetry properties of Ω. The present understanding of the RFI problem is hampered nowadays by some important dynamical effects, such as long-lived metastable states and irreversible processes, and by a number of unresolved questions and doubts related, for instance, to the existence of a "lower critical dimension" $d_{\rm LC}$ (which would imply that long-range order is destroyed below $d_{\rm LC}$, with perhaps $d_{\rm LC}=2$) or, more questionably, to some reported "dimensional reduction" [which would imply that the RFI model behaves like the $(d-\delta)$-dimensional pure Ising model]; there are even some doubts concerning the order of the involved phase transitions (which variously show up for different materials as first or second order, sometimes with very small values for the exponent β).[7-12] Summing up, the observation is difficult, the theory is scarce, and there are no final answers to the RFI problem, so that any related study such as the present one may be of some help.

The method we used in the analysis of the above questions is the Monte Carlo (MC) method. We actually performed a detailed finite-size-scaling analysis involving lattices $\Lambda=L\times L\times L$ with $L\leq 40$. Most data correspond to $L=40$; this case was treated with the most care, e.g., we discarded long initial evolutions before producing our equilibrium samples, these always were very large ones (e.g., 25 000 MC steps), say large enough to produce good Gaussians even for the fluctuations (i.e., specific heat and magnetic susceptibility), and we usually performed comparisons (eventually, averaging) between independent equilibrium samples corresponding to different initial configurations (these including at least initial configurations at zero and infinite temperatures). Some recent related Monte Carlo work, corresponding, however, to fields $\pm h$, may be found in Refs. 11 and 13; actually we adapted some of the technical computational methods described in Ref. 13, namely multispin coding and bit random number generators (see also Refs. 14 and 15).

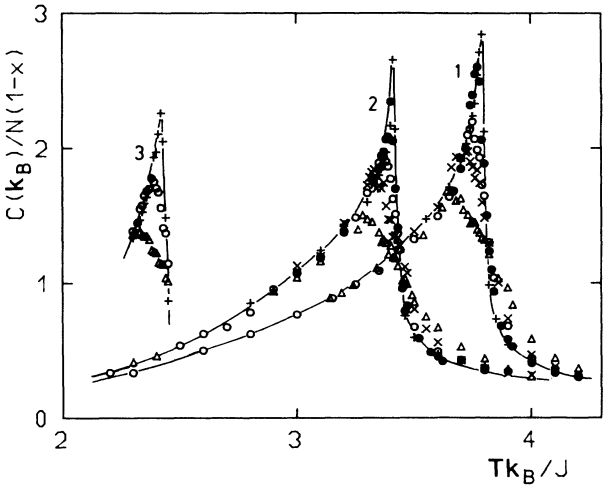

FIG. 2. The specific heat as a function of temperature for the cases 1, 2, and 3 (as indicated) defined in Sec. I. Different symbols correspond to different lattice sizes as follows: $L=8$ (△), 12 (×), 16 (○), 24 (●) and 40 (+).

Also noticeable is the fact that our restriction to relatively small defect concentration makes easier the application of the MC method, e.g., case 4 and its crossover to case 1 would be very difficult to study in practice for larger values of x.[4,13,16]

II. REGULARLY SPACED DEFECTS

The behavior of the specific heat for different values of L in cases 1–3 (cf. Fig. 2) and its comparison with the corresponding result for the pure, $x=0$ case[17] are most representative of the new situation. Figure 2 reveals in particular a well-defined maximum, which suggests a sharp divergence for the infinite lattice, occurring at T_c^L which differs for the three cases we considered. As for the pure case,[17] the height $C^L(T_c^L)$ increases and shifts towards larger temperatures with increasing L, and the values for T_c^L (which are given in Table I) follow rather accurately a linear behavior such that

$$T_c^L/T_c^\infty = a - bL^{-1/\nu}, \quad \nu=0.64\ , \tag{2.1}$$

for all the three symmetries with $a=0.9998$ and $b=1.1192$, i.e., we find essentially the pure behavior except that our value for b is slightly smaller than the one

TABLE I. The temperature (in units of k_B/J) locating the maximum of the specific heat in Fig. 2 for different lattice sizes.

L	Case 1	Case 2	Case 3
8	3.65±0.01	3.28±0.01	2.31±0.01
12	3.72±0.01	3.34±0.01	2.37±0.01
16	3.75±0.01	3.37±0.01	2.39±0.01
24	3.770±0.005	3.400±0.005	2.410±0.005
40	3.785±0.005	3.410±0.005	2.420±0.005

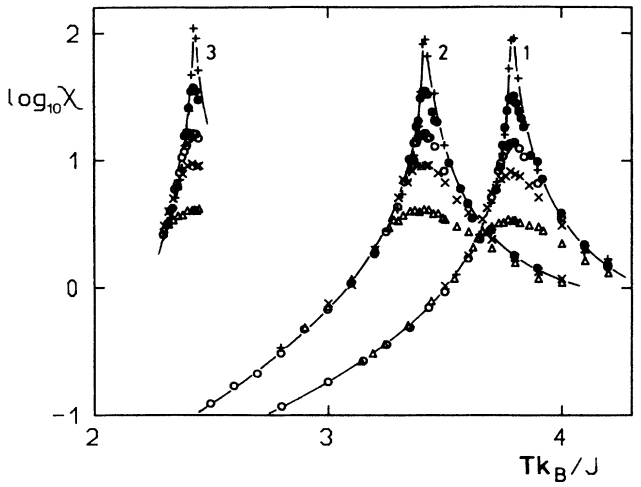

FIG. 3. Semilogarithmic plot of the magnetic susceptibility, as defined by Eq. (2.2), vs temperature. Same symbols are used as in Fig. 2.

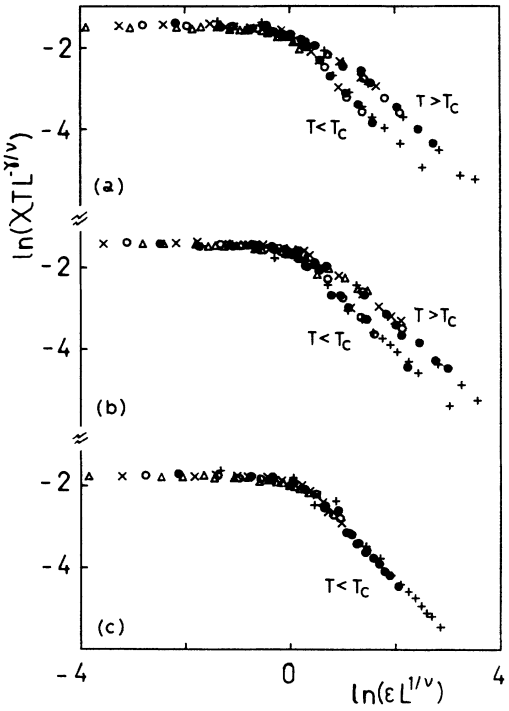

FIG. 4. The data in Fig. 3 plotted here scaled with the pure critical exponents values, $\gamma=1.25$ and $\nu=0.64$ and T_c^∞ as implied by Figs. 2 and 3 and by Eq. (2.1).

($b=1.4\pm0.2$) reported by Landau[17] for the pure case; probably such a discrepancy has no significance at all and one should consider $b=1.12\pm0.01$ as the value characterizing all the cases, pure and 1–3. The asymptotic values predicted by Eq. (2.1) are, respectively, $T_c^\infty k_B/J=3.797$, 3.421, and 2.431 for cases 1, 2, and 3.

The situation depicted by the specific heat is confirmed by the data for the magnetic susceptibility (cf. Fig. 3). This is defined here as

$$\chi=\frac{J}{k_B TN}\left[\left\langle\left[\sum_{x\in\Lambda}S_x\right]^2\right\rangle-\left\langle\left|\sum_{x\in\Lambda}s_x\right|\right\rangle^2\right], \qquad (2.2)$$

where $N=L^3$; the absolute value in the last term is included in order to avoid the counting as fluctuations of the hopping of the system (very near T_c^L) between states with a different sign for the magnetization (this is expected to be accurate enough when the system only employs a small fraction of the total time in that hopping.[18]) The comparison of the situation in Figs. 2 and 3 with the corresponding one in the pure case[17] strongly suggests, indeed, that the only changes for those regularly spaced defects occur in T_c^∞ which shows a dependence on x and symmetry. Actually, the finite-size scaling of χ^L with $\nu=0.64$, as in Fig. 4, produces the following values for the susceptibility critical exponents of the infinite system: $\gamma=1.24\pm0.04$ and $\gamma'=1.25\pm0.05$ for all three cases, in agreement with the values for the pure system, $\gamma=\gamma'=1.25$. [We obtain $C\approx0.4$ and $C'\approx0.2$ for the corresponding thermodynamic amplitudes. These values are, respectively, smaller and in agreement with the values for the pure system, $C\approx1.06$ and $C'\approx0.20$;[17] the discrepancy, however, seems just an artifact of our approximation (2.2), Ref. 16.] Also noticeable is the fact that the critical temperatures following from Figs. 3 and 4, as given by Table II, are in perfect agreement with the

TABLE II. Values for the critical temperature T_c and for the magnetization critical amplitude B as following from the study of the magnetization data (the differences observed in B may not be significative; see the text), and values for the critical energy as defined by Eq. (2.4), for the frustration parameter $\tilde{U}_c$ as defined by Eq. (2.5), and for the number of bonds between free spins (normalized to the value for the pure case), σ/σ_0. The cases 1–4 are defined in Sec. I (the latter is for $x=0.125$); the "blocking" cases $l=2,4$ are defined in Sec. III.

Case	T_c	B	U_c	σ/σ_0	$\tilde{U}_c$
1	3.797±0.001	1.55±0.05	0.278±0.004	0.75	0.371
2	3.422±0.001	1.52±0.05	0.363±0.004	0.75	0.484
3	2.432±0.001	1.49±0.05	0.270±0.004	0.50	0.540
4	2.8±0.1		0.61±0.04	$0.766=(1-x)^2$	0.80
Blocks					
$l=2$	3.585±0.005		0.352±0.005	0.758	0.465
$l=4$	3.400±0.005		0.440±0.02	0.765	0.57

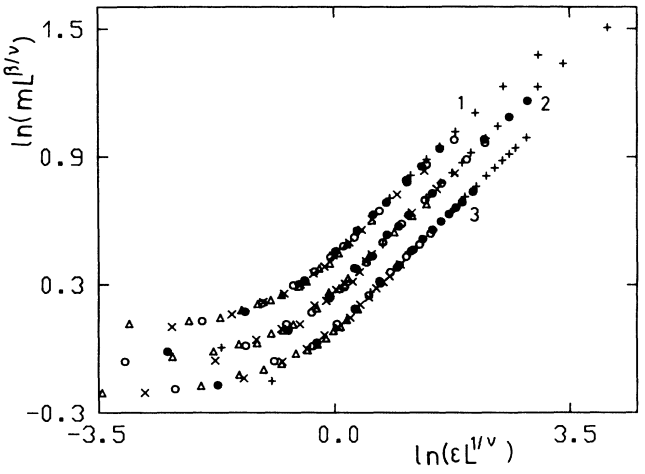

FIG. 5. Finite-size scaling of the magnetization data according to Eq. (2.30) with $\nu=0.64$ and $\beta=\frac{5}{16}$. Same symbols are used as in Fig. 2. The corresponding critical temperatures T_c^∞ were adjusted here to get the best scaling behavior; this produces the values given in Table II which are consistent with those in Table I and Eq. (2.1). For a better clarity of the graph, the magnetization for curve 1 was multiplied by the factor $(1-0.125)/(1-0.25)$. When one uses $m/(1-x)$ as an effective magnetization per (free) spin instead, all the data lies on the same curve.

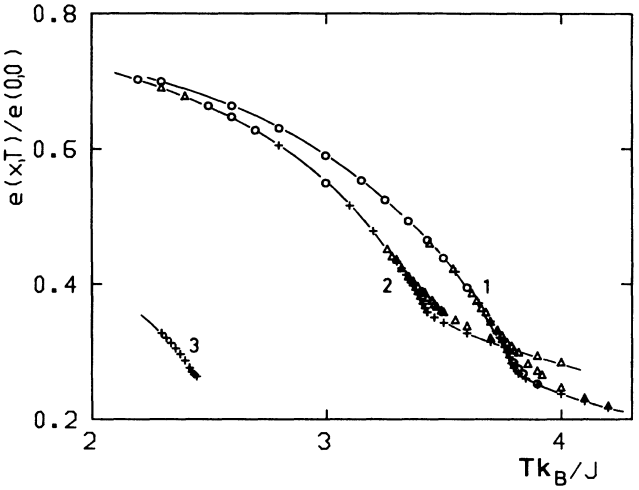

FIG. 6. The behavior of the system configurational energy with temperature for $L=8$ (△), 16 (○), and 40 (+), and for the three cases (as indicated) defined in Sec. I.

ones reported above obtained from Eq. (2.1).

Our main result above (second-order phase transition with pure critical exponents) is further confirmed with great accuracy by an independent finite-size-scaling study of the magnetization data which are even more precise than our data for the fluctuations (cf. Fig. 5). We find that

$$m(1-x)^{-1}=L^{-\beta/\nu}X^0(z),\quad z=\epsilon L^{1/\nu}\,, \tag{2.3}$$

where X^0 is the same for all three cases, and we were convinced by using different values for the set (β,ν,T_c^∞) that the best scaling occurs independently of x and symmetry for $\nu=0.64$, $\beta=0.31\pm0.005$, and T_c^∞ and the corresponding thermodynamic amplitudes B as given by Table II. That is, the values for T_c^∞ following here are quite consistent with the ones obtained from the previous analysis of fluctuations, and one should not discard that the amplitude has always the pure value $B=1.57$. We also find that the asymptotic value of $X^0(z)$ as $z\to0$ is 1.12 ± 0.05 for all three cases, in agreement with the pure value found by Landau.[17]

The behavior of the energy is depicted by Fig. 6, and the critical energy, defined as

$$U_c=\langle s_x s_y\rangle_c=e(x,T_c)/e(0,0)\,, \tag{2.4}$$

where $e(x,T)$ represents the configurational energy (1.1) when the defects concentration is x and the temperature is T, and $e(0,0)$ stands for the corresponding quantity for the pure model at zero temperature, is given by Table II. One has $U_c/(1-x)=0.318$, 0.415, and 0.360 for the critical energy per (free) spin in cases 1, 2, and 3, respectively. In order to interpret these values (as well as those in the tables) and gain further insight into the details of cases 1 to 3, one may notice the following.

The number of bonds between free spins, say σ (cf. Table II), is $0.75\sigma_0$, where σ_0 represents the same number for the pure system in cases 1 and 2, while $\sigma=0.5\sigma_0$ in case 3; more important, the nature of the bonds between free and fixed spins; $\sigma_0-\sigma$, essentially differs from one case to the other. That is, as shown by Fig. 1(a), every free spin having a fixed spin as a nearest neighbor (NN) in case 1 also has an NN fixed spin of the opposite sign, so that the $\sigma_0-\sigma$ free-fixed bonds give no net contribution to the total energy. Also, the symmetry is such in this case that the fixed spins (+ and −) should not introduce further net correlations than vacant sites.[4] Actually, the critical temperature we reported before for case 1 is consistent with the one for a dilute system with a concentration of $x=0.134$ $(=1-\sqrt{0.75})$ random nonmagnetic impurities as follows from the study in Ref. 4; of course, this fact does not exclude, however, other important differences between those two cases (the one in Ref. 4 and case 1 here). Concerning case 2 [cf. Fig. 1(b)], there are $0.25\sigma_0/3$ fixed (+)–free-fixed (−) bonds which give no net contribution to the system energy, and the rest, $0.25\sigma_0\frac{2}{3}$, are half free-fixed (+) and half free-fixed (−) bonds so that, assuming all the corresponding locations of the free spins are equivalent, they also give a zero net contribution to the energy. The free-fixed bonds, however, unlike the fixed–free-fixed ones, produce local NN correlations which, in spite of being globally compensated as in case 1, may locally induce frustration[19] leading to a critical temperature smaller than that for case 1 (corresponding, however, to the same concentration $x=0.125$). We shall report later on the observed dependence of the critical temperature on frustration for a given value of x. Case 3 [cf. Fig. 1(c)], on the other hand, is characterized

by fixed (+)–free-fixed (−), fixed (+)–free-fixed (+), and fixed (−)–free-fixed (−) bonds giving no net contribution to the global energy. The first class of bonds produce no correlations within each plane (there is again a great similarity with the case of vacant sites), while the others, which are perpendicular to those planes, favor the formation of clusters of aligned spins competing strongly with the surroundings at the interface thus causing a kind of frustration which is also present in case 2; in some sense the situation here is intermediate between those in cases 1 and 2.

In order to reflect quantitatively the preceding considerations, we may define

$$\tilde{U}_c = U_c \sigma_0/\sigma = \sigma_0 e(x, T_c)/\sigma e(0,0) , \tag{2.5}$$

which equals the minimum value of the correlation function between free spins, $\langle s_{\mathbf{x}} s_{\mathbf{y}} \rangle_c$, $\mathbf{x},\mathbf{y} \in \bar{\Omega}$, needed to form the ordered phase, and it can be interpreted as a frustration parameter. The values we obtain for $\tilde{U}_c$ (cf. Table II) reveal in particular that case 2 has a larger frustration than case 1, in spite of having both the same concentration of fixed spins.

III. RANDOM DISTRIBUTION OF DEFECTS

Case 4 is implemented in the computer by selecting at random the subsets Ω^+ and Ω^-, each containing $(x/2)L^3$ spins fixed at $+1$ and -1, respectively, out of Λ. The first observation here concerns the importance of finite-size effects. That is, while our previous study of nonmagnetic defects (i.e., vacant sites such that $s_{\mathbf{x}}=0$ when $\mathbf{x} \in \Omega = \Omega^+ \cup \Omega^-$) revealed that one may obtain results (even in a single large run) which are independent from the initial distribution of defects by using lattice sizes $L=30$ and 40,[3,4] a result which was confirmed afterwards by using larger lattices, $L=90$, in a larger computer,[14] our runs in the present case showed a definite dependence on the particular choices for Ω^+ and Ω^-. In order to minimize those effects, we were only concerned here with lattices $L=40$ (the largest size reasonably allowed by our computer) and systematically rejected any generated subset Ω lacking certain *a priori* spherical properties. Even so, we can only report on some qualitative properties of the system in case 4.

There is no doubt that every random choice Ω produces metastability and leads to an abrupt discontinuous phase transition like the ones reported in some RFI materials.[12] Also, an averaging of the data corresponding to independent distributions Ω does not seem to wash out the discontinuity though it tends to make it somewhat weaker (see Fig. 7). The corresponding transition temperature, which we can only estimate roughly (see later on for a description of our method), is around $Tk_B/J=2.8$ for $x=0.125$, and the frustration parameter is approixmately $\tilde{U}_c=0.80$. Thus, the frustration is now

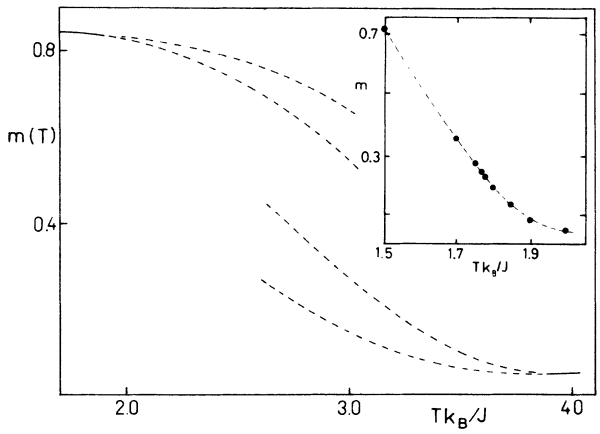

FIG. 7. Discontinuous phase transitions showed up by the model in case 4 (as defined in Sec. III) when $x=0.125$. The dashed lines in the main graph represent upper and lower bounds to the data obtained from different independent runs. The inset shows the situation when the concentration of fixed up spins is 0.049 53 and the one for fixed down spins is 0.050 47.

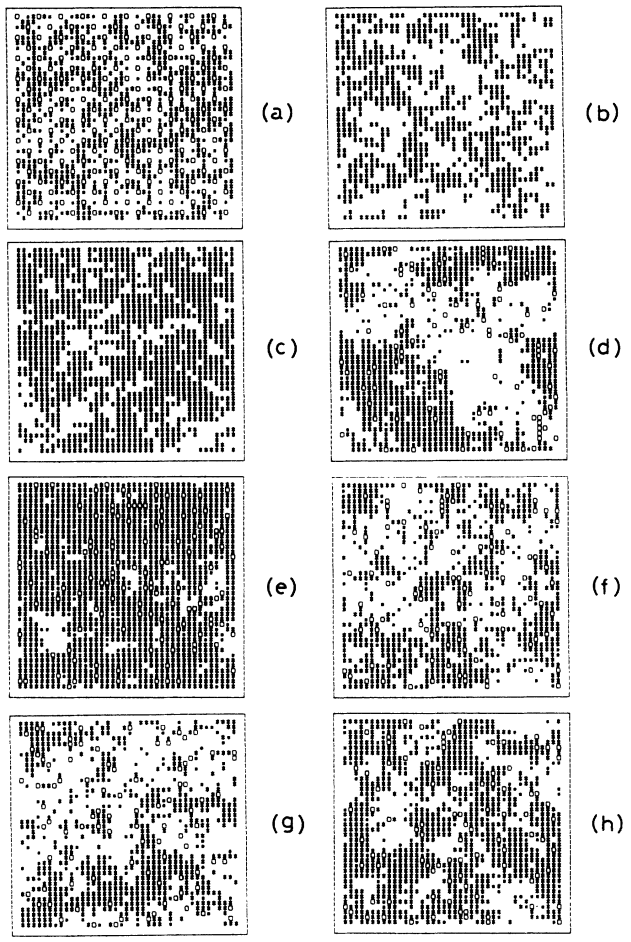

FIG. 8. Typical sections of the three-dimensional system configurations for different cases. Sometimes we show a plane with defects and an intermediate plane which contains no defects for the same system. The spin states are represented as follows: fixed up (□), fixed down (■), free up (*), and free down (no symbol). The cases shown are as follows: (a) case 1 for $T=1.1T_c$, (b) next plane for the same system, (c) case 1 for $T=0.97T_c$, (d) case 4 for $T=1.1T_c$, (e) case 4 for $T=0.96T_c$, (f) blocking $l=4$ for $T=1.1T_c$, (g) a different plane for the same system, and (h) blocking $l=4$ for $T=0.997T_c$.

much larger than before (cf. Table II). Actually, the system configurations near T_c (cf. Figs. 8) are here very different from those found for regularly spaced defects; for random Ω, the system shows up sometimes (e.g. in the metastability region) as segregated into two "infinite clusters," every one rich in one kind (up or down) of spin, while one may not distinguish those two clusters for ordered Ω, as one would expect for a continuous transition (cf. Figs. 8). Case 4 was also studied for $x=0.1$; we then found a first-order phase transition which is even more abrupt (i.e., a larger discontinuity) than for $x=0.125$ (notice that the latter case is probably rather near the corresponding "percolation" threshold as suggested by the fact that the frustration parameter then has a rather large value, $\tilde{U}_c=0.8$).

Another interesting observation for random Ω is the fact that the phase transition seems completely suppressed when Ω^+ and Ω^- contain a different number of (fixed) spins. This is illustrated by the inset in Fig. 7 corresponding to a system with 3170 spins fixed up and 3230 spins fixed down, both randomly located at a lattice $L=40$; that is, less than 0.1% of uneven fixed spins produce an extra field avoiding long-range order.

The rest of this section will be devoted to the study of the crossover *from case* 4, characterized by a discontinuous phase transition, *to case* 1, where the transition is second order. With that aim we partitioned the original lattice of side $L=40$ into n equal cubic boxes of side $l=Ln^{-1/3}$, and located at random a given number of fixed spins, actually xL^3/n fixed spins, inside each box. For $x=0.125$ we studied in detail the choices $n=8000$, $l=2$ (where a fixed spin is located randomly at each box with the restriction that the fixed spins at neighboring boxes have different sign), and $n=1000$, $l=4$ (where eight spins, half each sign, are located randomly at each box). Unlike in case 4, we found that the "blockings" with $l=2$ and $l=4$ show no dependence (for $L=40$ and equilibrium samples lasting some 25 000 MC steps) on the initial distribution of defects, a fact which was explicitly checked at each temperature; in order to obtain the best significant results and look for metastable states we also performed, as with the other cases, evolutions at each final temperature T starting from initial states corresponding to infinite and zero temperatures, respectively.

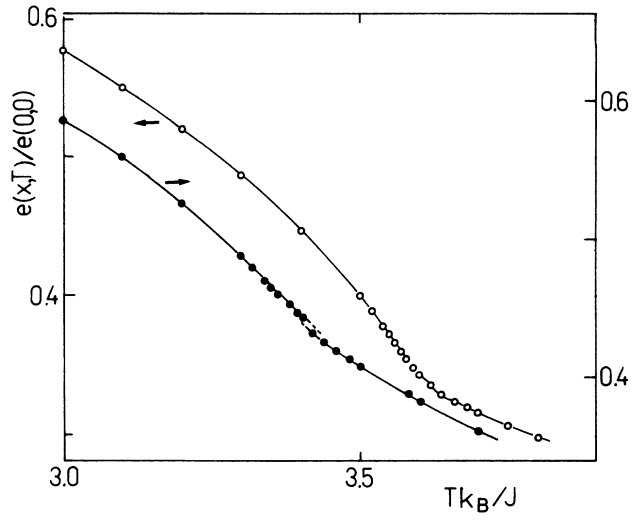

FIG. 9. The system configurational energy vs temperature for the blockings $l=2$ (○) and $l=4$ (●) described in Sec. III. Notice the shift in the respective scales.

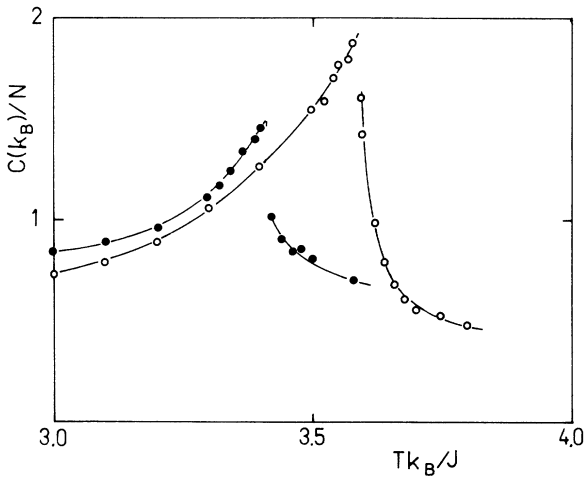

FIG. 10. Behavior of the specific heat for the same systems as in Fig. 9.

The behavior of the resulting energy is depicted by Fig. 9. The case $l=4$ reveals a weak discontinuity (which is hardly distinguishable for $l=2$) to be confirmed below. Otherwise, the situation resembles somewhat that for regularly spaced defects, e.g., we find (cf. Table II) $\tilde{U}_c=0.465$ for $l=2$, which is very cose to the value found for case 2, and $\tilde{U}_c=0.57$ for $l=4$, which reveals a larger frustration than for the other ordered cases. The specific heat is represented in Fig. 10. This, in addition to locating the transition temperature as given by Table II, reveals a behavior qualitatively different from that in Fig. 2; i.e., instead of the rapid increase near T_c in Fig. 2 suggesting a divergence for the infinite lattice, the data in Fig. 10, rather, suggest a discontinuous jump which

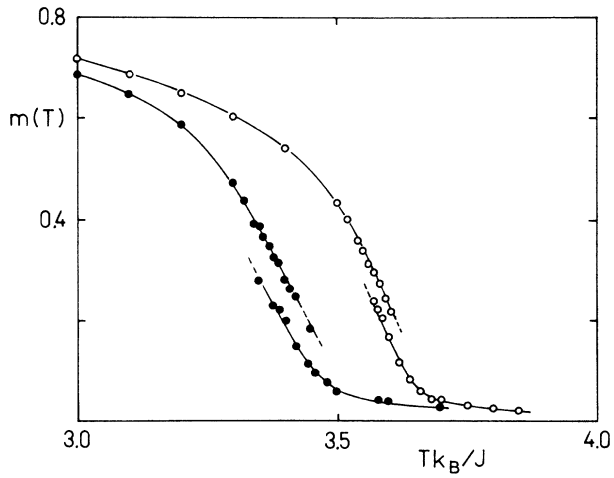

FIG. 11. The magnetization data for the same systems as in Fig. 9.

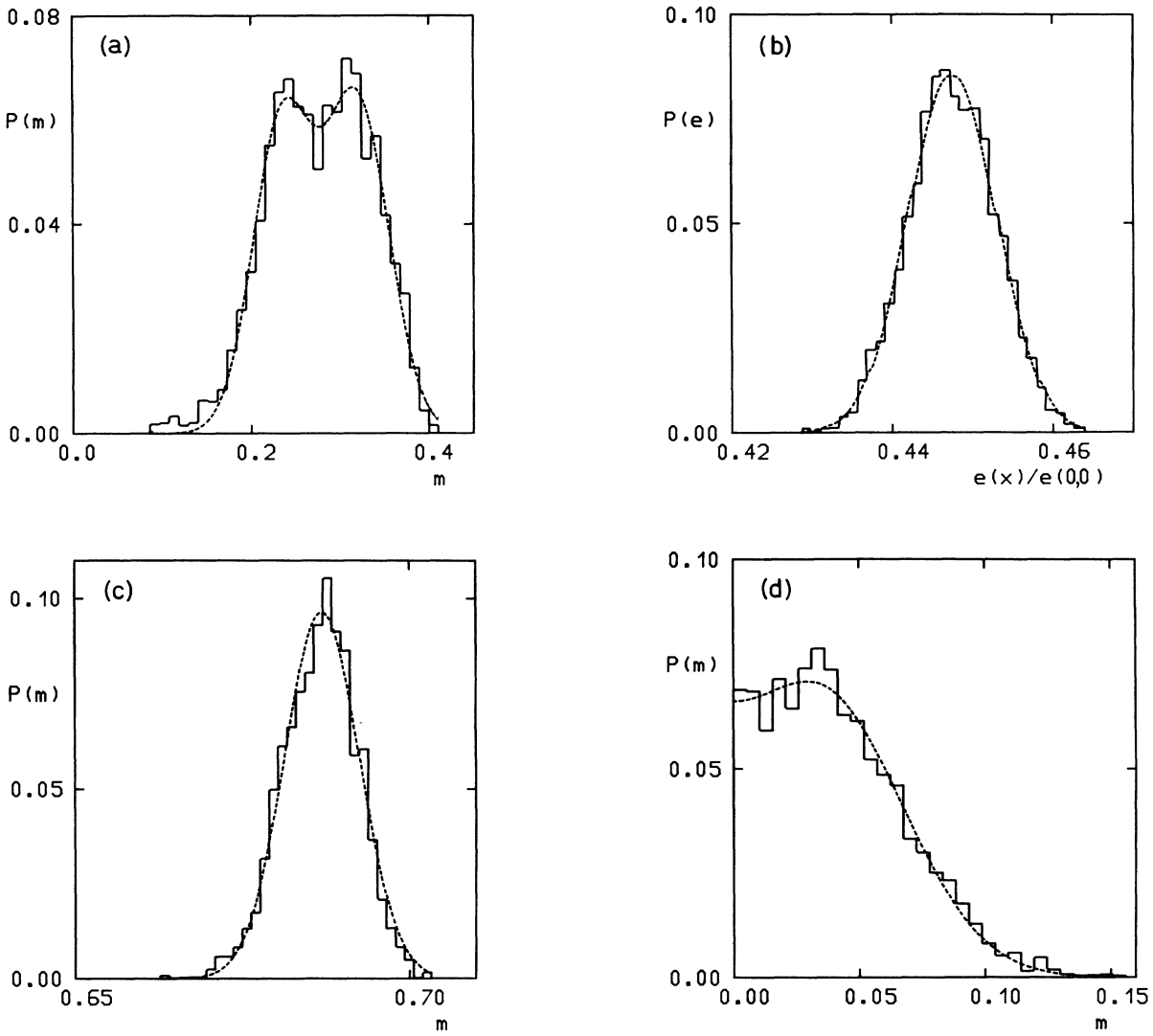

FIG. 12. Distribution of measured values and fitted Gaussians for the "blocked" system with $l=4$: (a) magnetization values for $T=0.997\ T_c$, (b) energy values for the same temperature, (c) magnetization values for $T=0.882T_c$, and (d) magnetization values for $T=1.058T_c$.

characterizes a first-order phase transition. This is further confirmed by the magnetization data in Fig. 11 where the discontinuity is evident; also, the transition temperatures implied by the location of the maxima of the specific heat, as given by Table II, agree with the temperatures locating the middle of the regions in Fig. 11 for which we found distinct states when the system is heated up from a zero-temperature condition or it is quenched down from an infinite temperature condition. It also seems interesting to mention that our energy and magnetization values for equilibrium and metastable states were obtained, as illustrated by Fig. 12, by adjusting the distribution of the different measured values to two Gaussians. In the case of the energy for all considered temperatures, and for the magnetization well below the transition temperature, both Gaussians superimpose; very near T_c, however, equilibrium and metastable states are energetically very close to each other and the system magnetization hops from one to the other. This effect is rather clear when one compares Figs. 12(a) and 12(b) for the magnetization and energy raw data, respectively, at the same ($0.997T_c$) temperature. The raw data in Fig. 12(c), on the contrary, define a unique (equilibrium) segregated state at $0.882T_c$, and Fig. 12(d) shows the expected, qualitatively different situation slightly above T_c.

IV. CONCLUSIONS

We have studied the three-dimensional ferromagnetic Ising model with quenched fixed spin defects as it may be relevant to analyze the influence of the defect distribution symmetry on the nature of the phase transition, and relevant to the investigation of the random field[7,8] and frustrated[19] Ising problems. Our main conclusion is that, while regularly spaced defects lead to a well-defined second-order phase transition with pure Ising critical exponents, so that there is no dimensional reduction[8] in

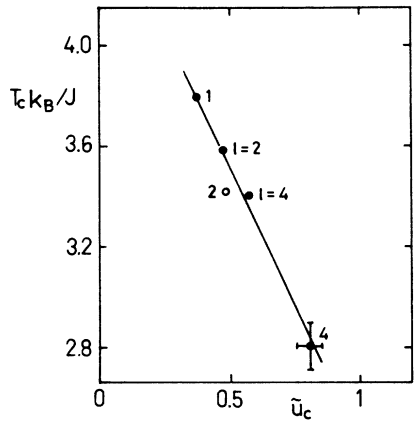

FIG. 13. Transition temperature vs frustration parameter when the symmetry is essentially the same (●) and for different symmetries (○). The line fitting the solid circles is $y=4.52-2.09\tilde{U}_c$; this is not expected to be valid outside the $\tilde{U}_c$ range investigated. Case 3, also deviating from that linear behavior, is not shown in order to obtain a better detail.

that case, any randomness in the distribution of defects changes the transition from second to first order, the discontinuities apparently being very abrupt for a completely random defect distribution. Abrupt discontinuities, and second-order transitions with small values for the exponent β, thus resembling first-order transitions, have also been reported for some RF systems.[11,12] When the magnetization added by the defects is nonzero, however, the phase transition is suppressed; this could perhaps explain the apparent existence of a lower critical dimension larger than the one in some experiments.[7] It also raises some doubts about the dimensional reduction concept, in agreement with recent trends.[20] On the other hand, when the system has a well-defined transition temperature, this seems to behave approximately linearly with our frustration parameter (2.5), within the $\tilde{U}_c$ range investigated here, for a given defects symmetry and concentration x; this is illustrated by Fig. 13. Note also that for the defects concentration we have considered, namely for $x=0.1$, 0.125, and 0.25, there are no dynamical problems or fluctuating interfaces[13] preventing the system from reaching the equilibrium or the expected metastable states. Finally, it is noticeable that the global situation here is, in particular, very different from the one found in the case of dilute Ising models.[4,18]

ACKNOWLEDGMENTS

Partially supported by the CAICYT, Spain, Grant No. PB85/0062, and by the Comité Conjunto Hispano-Norteamericano, Project No. CCB-8402/025.

[1]A. Labarta, J. Marro, and J. Tejada, J. Phys. C **19**, 1567 (1986).
[2]A. Labarta, J. Marro, and J. Tejada, J. Magn. Mater. **57**, 54 (1986).
[3]J. Marro, A. Labarta, and J. Tejada, Phys. Rev. B **34**, 347 (1986).
[4]A. Labarta, J. Marro, and J. Tejada, Physica **142B**, 31 (1986).
[5]M. E. Fisher and H. Au-Yang, J. Phys. C **8**, L418 (1975), and references therein.
[6]M. E. Issigoni and C. Papatriantafillon, J. Stat. Phys. **45**, 527 (1986).
[7]G. Grinstein, J. Appl. Phys. **55**, 2371 (1984).
[8]Y. Imry, J. Stat. Phys. **34**, 849 (1984).
[9]D. P. Belanger, A. R. King, and V. Jaccarino, J. Appl. Phys. **55**, 2383 (1984). See D. P. Belanger, A. R. King, and V. Jaccarino, Phys. Rev. B **34**, 452 (1986); W. Kleemann, A. R. King, and V. Jaccarino, *ibid.* **34**, 479 (1986); J. A. Mydosh, A. R. Kingaud, and V. Jaccarino, J. Magn. Magn. Mater. **54-57**, 47 (1986); C. Magon, J. Sartorelli, A. R. King, V. Jaccarino, M. Itoh, H. Yasuoka, and P. Heller, *ibid.* **54-57**, 49 (1986), for instance, for some related experimental work.
[10]A. Aharony, Phys. Rev. B **18**, 3318 (1978).
[11]A. P. Young and N. Nauenberg, Phys. Rev. Lett. **54**, 2429 (1985); A. T. Ogielski, *ibid.* **57**, 1251 (1986).
[12]R. J. Birgeneau, R. A. Cowley, G. Shirane, and H. Yoshizawa, Phys. Rev. Lett. **54**, 2147 (1985).
[13]D. Stauffer, C. Hartzstein, K. Binder, and A. Aharony, Z. Phys. B **55**, 325 (1984).
[14]D. Chowdhury and D. Stauffer, J. Stat. Phys. **44**, 203 (1986).
[15]S. Kirkpatrick and E. P. Stoll, J. Comp. Phys. **40**, 517 (1981).
[16]D. P. Landau, Physica **86-88B**, 731 (1977); Phys. Rev. B **22**, 2450 (1980).
[17]D. P. Landau, Phys. Rev. B **14**, 255 (1976).
[18]See, for instance, O. G. Mouritsen, *Computer Studies of Phase Transitions and Critical Phenomena* (Springer-Verlag, Berlin, 1984).
[19]See, for instance, R. Liebmann, *Statistical Mechanics of Periodic Frustrated Ising Systems* (Springer-Verlag, Berlin, 1986).
[20]J. Villain, J. Phys. (Paris) **46**, 1843 (1985).